

# Self-reinforcement in Li- $\alpha$ -sialon ceramics

Z. B. YU, D. P. THOMPSON

*Materials Division, Department of Mechanical, Materials and Manufacturing Engineering, University of Newcastle upon Tyne, NE1 7RU, UK*

A. R. BHATTI

*Structural Materials Centre, DERA Farnborough, Hampshire, GU14 0XL, UK*

Self-reinforcement of Li- $\alpha$ -sialon ceramics by *in situ* growth of elongated  $\alpha$  and  $\beta$ -sialon grains has been explored and analysed. Properties of Li- $\alpha$ -sialon ceramics are mainly determined by the overall starting composition and the crystalline modification of the starting  $\text{Si}_3\text{N}_4$  powder which in turn determine the final microstructure of the materials. Both the morphology and crystalline phase of the elongated sialon grains have strong effects on the toughening mechanism. The results indicate that  $\alpha$ -sialons reinforced by elongated  $\beta$ -sialon grains have advantages over similar materials reinforced by elongated  $\alpha$ -sialon grains because of the type of crack deflection toughening mechanism involved.

© 2001 Kluwer Academic Publishers

## 1. Introduction

Self-reinforced ceramics are defined as materials having the ability to produce microstructures *in situ* with unique micro-morphologies that allow toughening mechanisms to take place [1]. Self-reinforced ceramics usually have microstructures in the form of either sphere-, rod- or plate-like grains, which can change the way a crack propagates either along interface boundaries or by deflection etc; in this way self-reinforced ceramics have more flaw-tolerance than normal equiaxed monolithics. Generally, self-reinforced ceramics are limited to specific systems and the improvement in fracture toughness ranges typically from 1.5 to 4 times that of monolithic materials depending on the final microstructure and what shapes of grains are present [2, 3]. Although the improvement in fracture toughness is not as impressive as for second phase reinforced materials, nevertheless, considering the difficulties encountered in developing two phase structures such as whisker and fibre reinforced ceramics, one of the advantages of the self-reinforcement method is the simpler processing involved.

Self-reinforced ceramics can be formed either in oxide systems ( $\text{Al}_2\text{O}_3$  [4], mullite,  $\text{Al}_2\text{O}_3\text{-ZrO}_2$ ,  $\text{MgO-CaO}$  [5] or non-oxide systems ( $\text{Si}_3\text{N}_4$ , sialon,  $\text{AlN}$ ,  $\text{AlN-SiC}$ ) [6–8]. For  $\alpha$ -sialon ceramics, there are two types of self-reinforcement, namely:

(1) simultaneous crystallisation of two-phase  $\alpha/\beta$ -sialons using a eutectic composition liquid, from which it has been demonstrated that the phase ratio can be controlled just by changing the overall composition [9, 10]. According to these observations, extensive work has been focused on the design of  $\alpha/\beta$ -sialon ceramics which combine the strength and fracture toughness of  $\beta$ -sialon and the hardness of  $\alpha$ -sialon to give a tailored combination of mechanical properties. However, re-

cently the discovery of reversible *in situ* transformation between  $\alpha$ - and  $\beta$ -sialon in some rare sialon systems [9–12] imposes limitations on these ceramics as high temperature structural materials.

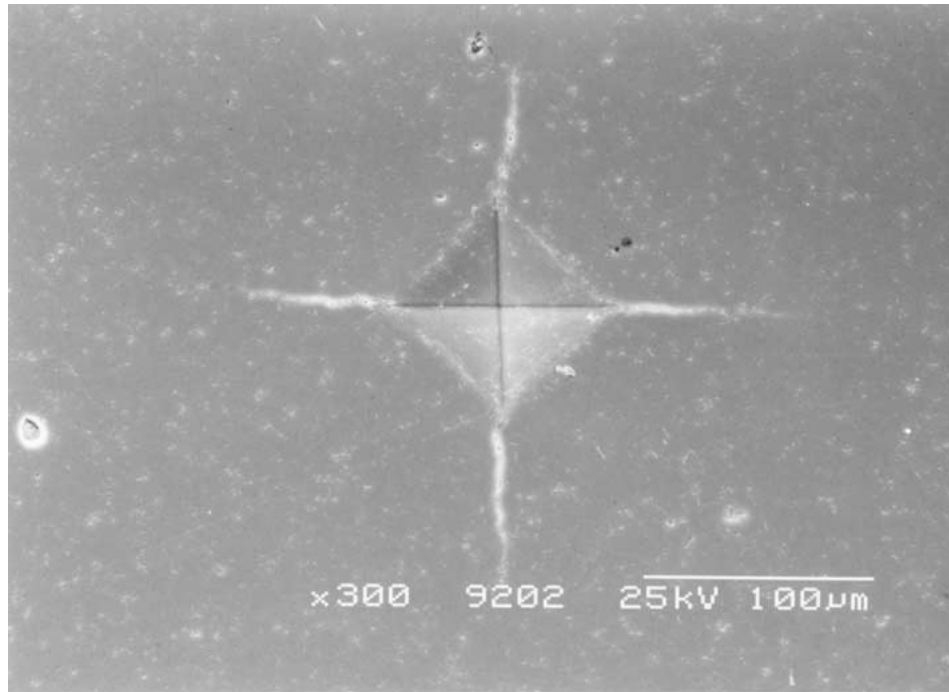
(2) direct growth of elongated  $\alpha$ -sialon grains in dense  $\alpha$ -sialon ceramics. It has been observed that dense  $\alpha$ -sialon ceramics containing elongated grains can be prepared by carefully selecting the starting composition [13–17]. For instance, Chen *et al.* [16] demonstrated that elongated  $\alpha$ -sialon grain could be achieved in a dense  $\alpha$ -sialon matrix by using high  $\beta$ - $\text{Si}_3\text{N}_4$  starting powder and got a fracture toughness comparable to that of  $\beta$ -sialon whilst at the same time keeping the advantage of the high hardness of  $\alpha$ -sialon (20–22 GPa).

Self-reinforcement is actually based on the principle that the main toughening contribution comes from mechanisms such as debonding, crack bridging, pull-out and crack deflection [18]. Obviously, the morphology of *in situ* formed elongated grains in the final microstructure has the major effect on self-reinforcement. However, other factors such as interfacial bonding, interface morphology, strength and aspect ratio of elongated grains also have a strong impact on the debond zone and crack deflection [19, 20]. It should be noted that residual stress due to thermal and/or elastic modulus mismatches play an important role in elongated-grain reinforcement of  $\alpha$ -sialon ceramic matrix composites. In order to take full advantage of self-reinforcement, the chemical and especially the physical compatibility between the phases with different morphologies in the final microstructure should also be carefully considered and designed because the type and magnitude of internal stresses at the grain boundaries are determined by the thermal expansion and by elastic mismatches between the different phases, which in turn have a strong effect on crack propagation.

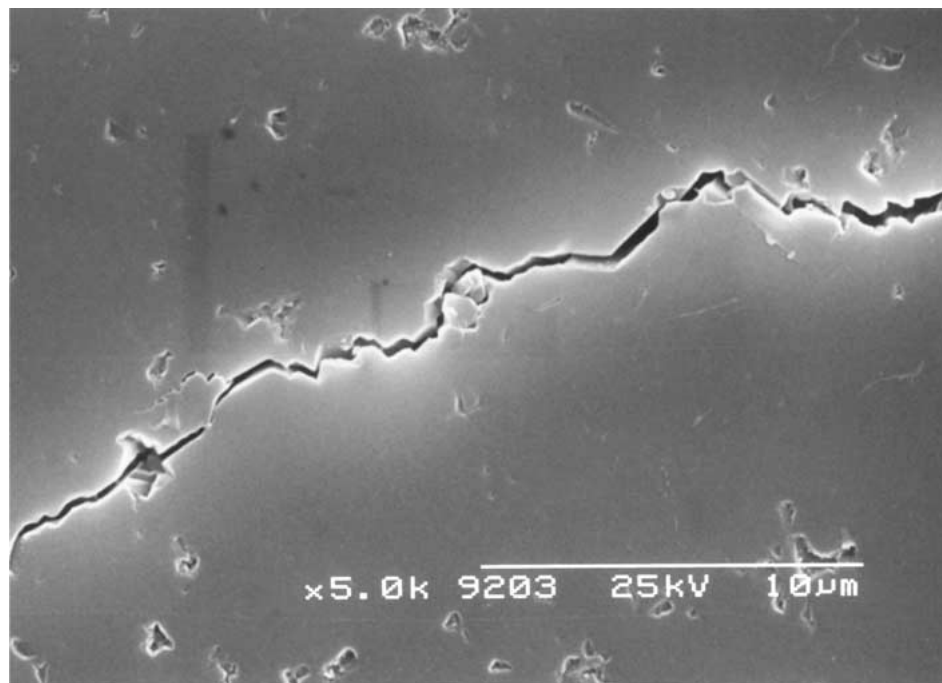
In the present paper, an equiaxed  $\alpha$ -sialon matrix reinforced with *in situ* formed elongated  $\alpha$ - and  $\beta$ -sialon grains has been investigated; the effects of grain size, chemical composition of the grains and the grain boundary phases on crack propagation are discussed; factors such as aspect ratio ( $L/D$ ) and the thermal and Young's modulus mismatch between phases with different grain morphologies on the toughening mechanism have been analysed. Li cation stabilised  $\alpha$ -sialons have been studied in this work because it is one of a series of studies [12, 17, 21] carried out in Newcastle on Li- $\alpha$ -sialon ceramics.

## 2. Experimental procedure

Two types of  $\text{Si}_3\text{N}_4$  powder were used, one an  $\alpha$  rich  $\text{Si}_3\text{N}_4$  powder (H.C. Starck, Grade B7), containing 90% of  $\alpha$  phase; the other a  $\beta$  rich  $\text{Si}_3\text{N}_4$  powder (AME), containing 64% of  $\beta$  phase. Other materials were  $\text{Al}_2\text{O}_3$  (BDH);  $\text{AlN}$  (H.C. Starck Grade B);  $\text{Li}_2\text{CO}_3$  (99%, BDH);  $\text{SiO}_2$ , (Precipitated, BDH). When calculating the composition of the samples, corrections were made for the residual oxygen content of  $\text{Si}_3\text{N}_4$  and  $\text{AlN}$ . The samples were fabricated by hot-pressing as described previously [17, 21].



(a)



(b)

Figure 1 SEM micrographs of indentation (a), crack propagation (b) and multiphase  $\alpha/\beta$  sialon grains (c) in the (0.5, 2.0) sialon sample showing the toughening role of elongated  $\beta$ -sialon grains (Continued).



(c)

Figure 1 (Continued).

Phase analysis of the crushed powders was measured using a Guinier-Hägg focusing X-ray camera with Si as internal standard; bulk surfaces polished parallel and perpendicular to the hot pressing direction were examined by diffractometry with Ni filtered Cu  $K_{\alpha}$  radiation. Room temperature Vickers hardness measurements were made on mounted and polished samples using a pyramidal diamond indenter (Crayford, Kent). The standard procedure was to apply a load ( $P$ ) of 10 kg for 10 seconds. At least five indentations were made for each sample. The Vickers hardness ( $H_v$ ), and fracture toughness ( $K_{IC}$ ) were calculated using the expression given by Evans *et al.* [22] as:

$$H_v(\text{kg/mm}^2) = \frac{0.47P}{a^2} \quad (1)$$

$$K_c(\text{MPam}^{1/2}) = \frac{0.15k(c/a)^{-3/2}H_v g \sqrt{a}}{\phi} \quad (2)$$

where  $H_v$  is the Vickers hardness ( $\text{kg/mm}^2$ ),  $P$  is the applied force and  $a$  is half the length of the diagonal indentation produced by the diamond.  $K_{IC}$  is the fracture toughness ( $\text{MPam}^{1/2}$ ),  $\Phi$  is the constraint factor ( $\approx 3.0$ ),  $g$  is the gravitational acceleration ( $9.81 \text{ m/s}^2$ ),  $c$  is the average length of the radial cracks, and  $k$  is a correction factor ( $\approx 3.2$  for large  $c/a$  values). The accuracy of the value obtained for  $K_c$  is believed to be  $\approx 30\%$ .

Microstructural observations of indentations in polished and etched samples and fracture surfaces were carried out on an S-2400 Scanning Electron Microscope, with polished samples etched by immersion in hot molten KOH for 30 min. All samples were either carbon or gold coated prior to SEM observation to avoid electron charging.

Six compositions were chosen for study in this work, including two-phase  $\alpha/\beta$  sialon and single-phase

TABLE I Compositions of Li- $\alpha$ -sialon ( $\text{Li}_x\text{Si}_{12-(m+n)}\text{Al}_{(m+n)}\text{O}_n\text{N}_{16-n}$ ) used in this study

Sample	$m$	$n$	$x$
$(0.5, 2.0)_{\alpha}$	0.5	2.0	0.5
$(1.0, 1.0)_{\alpha}$	1.0	1.0	1.0
$(1.0, 1.0)_{\beta}$	1.0	1.0	1.0
$(1.0, 2.0)_{\alpha}$	1.0	2.0	1.0
$(1.0, 2.0)_{\beta}$	1.0	2.0	1.0
$(2.0, 2.0)_{\alpha}$	2.0	2.0	2.0

$\alpha$ -sialons with different compositions for comparison; these are listed in Table I.

### 3. Results and discussion

#### 3.1. Microstructure and property

Table II lists the hardness and fracture toughness of various samples. As Table II shows, the multiphase (0.5, 2.0) sample showed a higher fracture toughness but a lower hardness; the higher fracture toughness is because of the substantial amount of *in situ* growth of whisker-like  $\beta$ -sialon grains (see Fig. 1c). These grains make a significant contribution to the fracture

TABLE II Mechanical properties of  $\alpha$ -sialons of different compositions

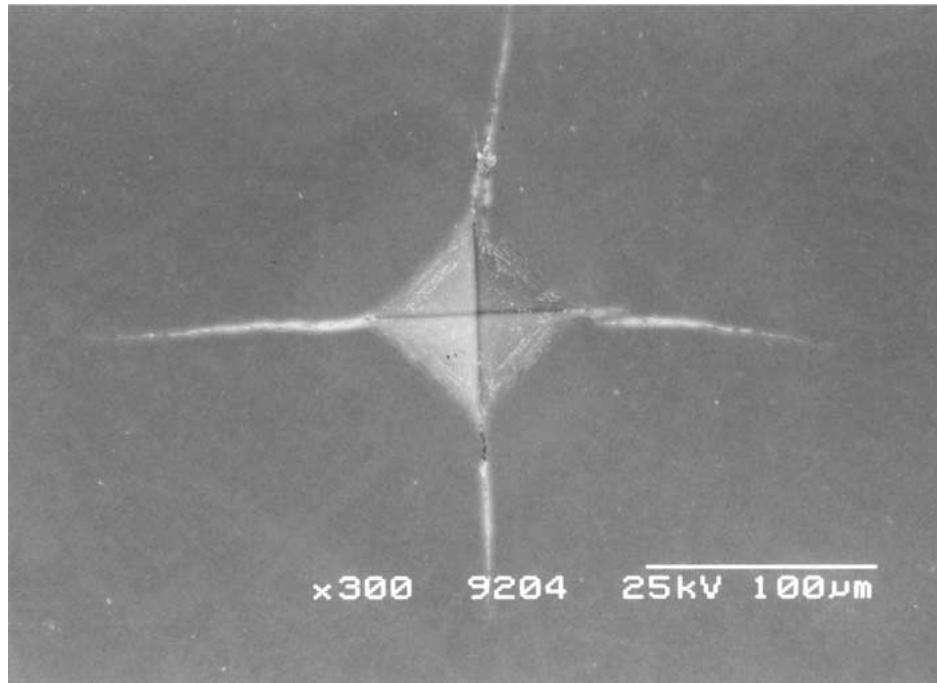
Composition ( $m, n$ )	Starting powder	$\alpha'/\beta'$ ratio	$H_{V10}$ (GPa)	$K_{IC}$ ( $\text{MPam}^{1/2}$ )
(0.5, 2.0)	$\alpha$	41/59	$17.9 \pm 0.5$	$6.8 \pm 0.5$
(1.0, 1.0)	$\alpha$	100/0	$20.3 \pm 0.4$	$4.9 \pm 0.3$
(1.0, 1.0)	$\beta$	100/0	$20.2 \pm 0.9$	$4.2 \pm 0.4$
(1.0, 2.0)	$\alpha$	100/0	$18.3 \pm 0.5$	$5.0 \pm 0.4$
(1.0, 2.0)	$\beta$	100/0	$18.0 \pm 0.2$	$4.4 \pm 0.3$
(2.0, 2.0)	$\alpha$	100/0	$15.3 \pm 0.7$	$4.7 \pm 0.7$

toughness. Micrographs of indentation and crack propagation in this sample are shown in Fig. 1a and b, and indicate that crack bridging and especially crack deflection are the main processes operating during crack propagation in this material.

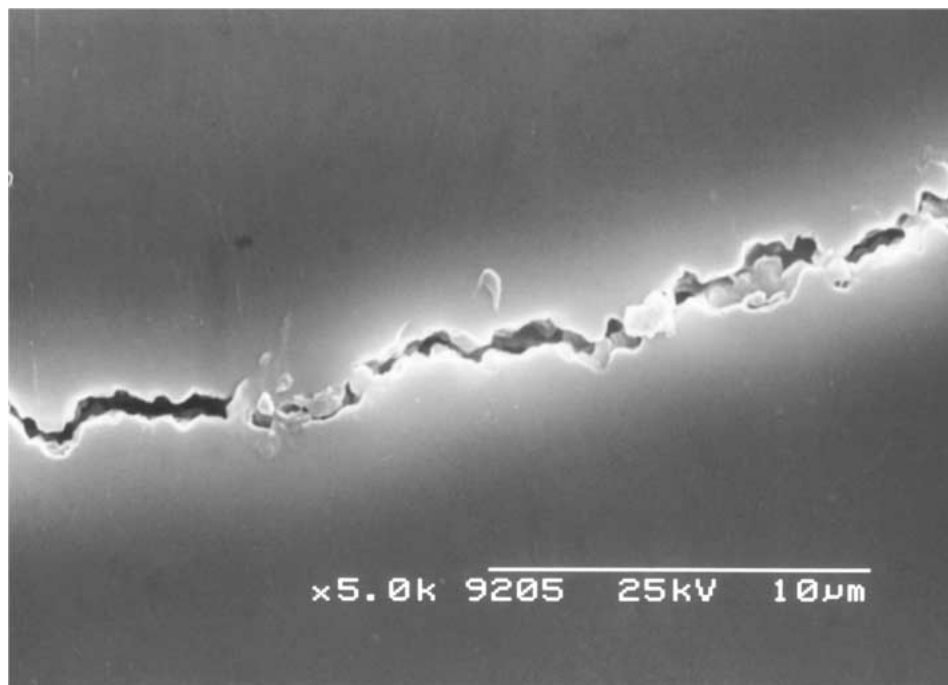
For pure  $\alpha$ -sialon ceramics, the properties depend on their compositions. For instance, (1.0, 1.0) samples, consisting of only equiaxed grains and with a very small amount of residual glassy phase, have very high hardness ( $\sim 20$  GPa) but a lower fracture toughness. However, (1.0, 2.0) samples, containing a large amount of equiaxed grains, a small proportion of elongated

$\alpha$ -sialon grains and a very small amount of glassy phase, have a relatively low hardness ( $\sim 18$  GPa) but a higher fracture toughness compared with (1.0, 1.0) samples.

It should be noted that the starting powder has an obvious effect on the fracture toughness but not on the hardness. As shown in Table II, though the hardness values are similar, samples of the same composition made from  $\alpha$  rich  $\text{Si}_3\text{N}_4$  starting powder have a higher fracture toughness than those made from  $\beta$  rich  $\text{Si}_3\text{N}_4$  starting powder. The reason is perhaps that the  $\beta$ - $\text{Si}_3\text{N}_4$  starting powder generates a microstructure with coarser grains and a relatively larger amount of grain boundary

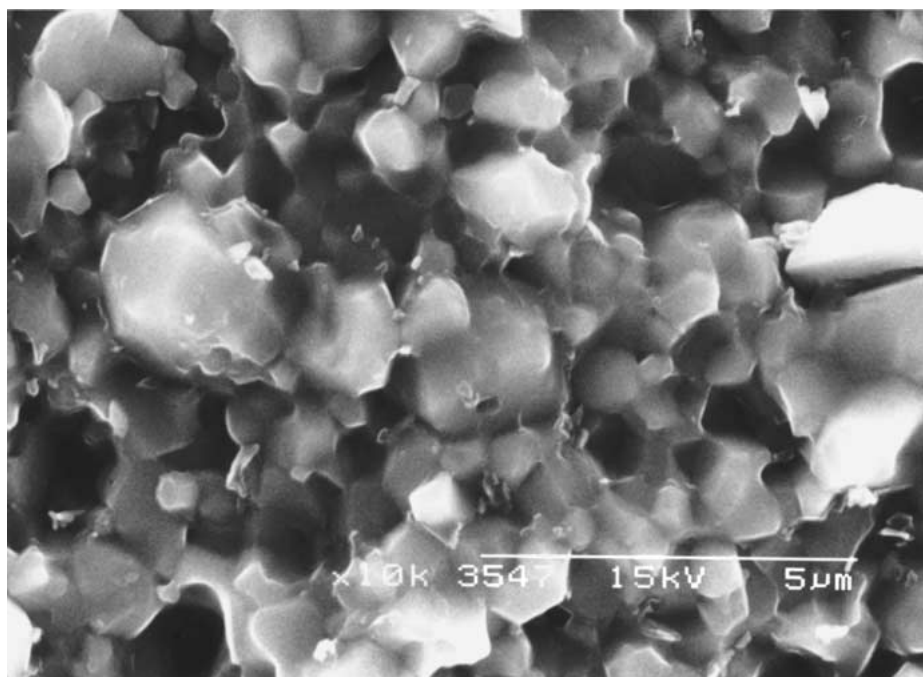


(a)



(b)

Figure 2 SEM micrographs of indentation (a), crack propagation (b) and fracture surface (c) in the (1.0, 1.0) sample made from  $\alpha$  rich  $\text{Si}_3\text{N}_4$  starting powders (Continued).



(c)

Figure 2 (Continued).

phase; in contrast, the  $\alpha$  rich  $\text{Si}_3\text{N}_4$  starting powder results in finer grains with much less grain boundary phase, i.e. a cleaner grain boundary. This has been further confirmed by the fact that the samples made from  $\beta$  rich  $\text{Si}_3\text{N}_4$  starting powder are more easily etched than those made from  $\alpha$  rich  $\text{Si}_3\text{N}_4$  starting powder [17]. The difference in microstructure leads to a different type of crack propagation. As shown in Fig. 2a and b, in the  $(1.0, 1.0)_\alpha$  sample, cracks propagate in a complicated zigzag way suggesting that propagation of the crack is along grain boundaries, i.e. inter-granular fracture. It can be seen clearly that some bridging, deflection and even pullout occurred in the sample because of the very thin grain boundary film. The fracture surface (Fig. 2c) is quite rough and also shows massive regular facet holes indicating that a substantial proportion of the equiaxed particles have been pulled out, resulting in a high work of fracture during crack propagation, so this material shows a relatively higher fracture toughness. This might suggest an alternative method for self-reinforcement of pure  $\alpha$ -sialon ceramics with a microstructure consisting of very fine grains and clean grain boundaries. However, in the  $(1.0, 1.0)_\beta$  sample, the propagation of the crack is fairly straight and smooth, and neither deflection nor bridging occurred suggesting that an intragranular fracture is the main process during crack propagation (see Fig. 3a and b). Fig. 3c shows a relatively smooth fracture surface which further confirms that intragranular fracture occurred in this material.

Chemical composition also has a strong effect on mechanical properties, since the starting composition directly affects the microstructure of these materials, which in turn determines their properties. For example, crack propagation in the  $(1.0, 1.0)_\beta$  sample and in the  $(1.0, 2.0)_\beta$  sample is totally different because of the different microstructure (see Fig. 3c and Fig. 4c).

Since both  $(1.0, 2.0)$  samples contain some elongated  $\alpha$ -sialon grains, crack propagation in these samples (Figs 4a and 5a) indicates that self-reinforcement by toughening mechanisms such as debonding, deflection and pullout occurred in these samples. Therefore, the fracture toughness of the both  $(1.0, 2.0)$  samples are higher than the corresponding  $(1.0, 1.0)$  samples. So, just as with whisker-reinforced ceramic composites, it can be expected that the fracture toughness of pure  $\alpha$ -sialon could be further improved if the amount and especially the aspect ratio ( $L/D$ ) of elongated  $\alpha$ -sialon grains could be further increased by accurately designing the chemical compositions and carefully controlling the processing parameters.

### 3.2. Factors affecting the toughening of $\alpha$ -sialons with *in situ* formed elongated grains

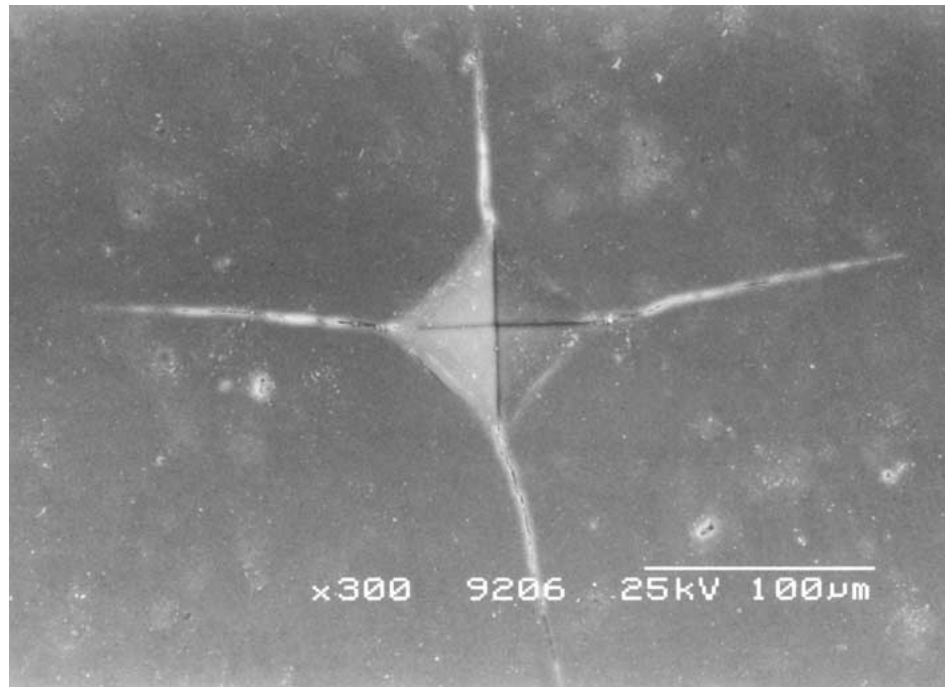
As shown above, crack deflection is the main toughening mechanism involved in Li- $\alpha$ -sialon ceramics containing *in situ* formed elongated grains. Crack deflection usually involves two types of deflection: tilting of the crack about an axis parallel to the crack front, and twisting about an axis normal to the crack front. The change in orientation of the crack plane during deflection leads to a reduction in the crack extension force. The mechanism of crack deflection was analysed by Faber and Evans [2, 3] by evaluating the mixed mode stress intensity factors in the deflected region. Their results showed that for a random array of obstacles the toughening increment depends on the volume fraction and the shape of the particles.

It should be noticed that, in the present work, the *in situ* reinforcement of Li- $\alpha$ -sialon ceramics by elongated  $\alpha$  and  $\beta$  grains is different although crack deflection occurs in both cases. This is because deflection can

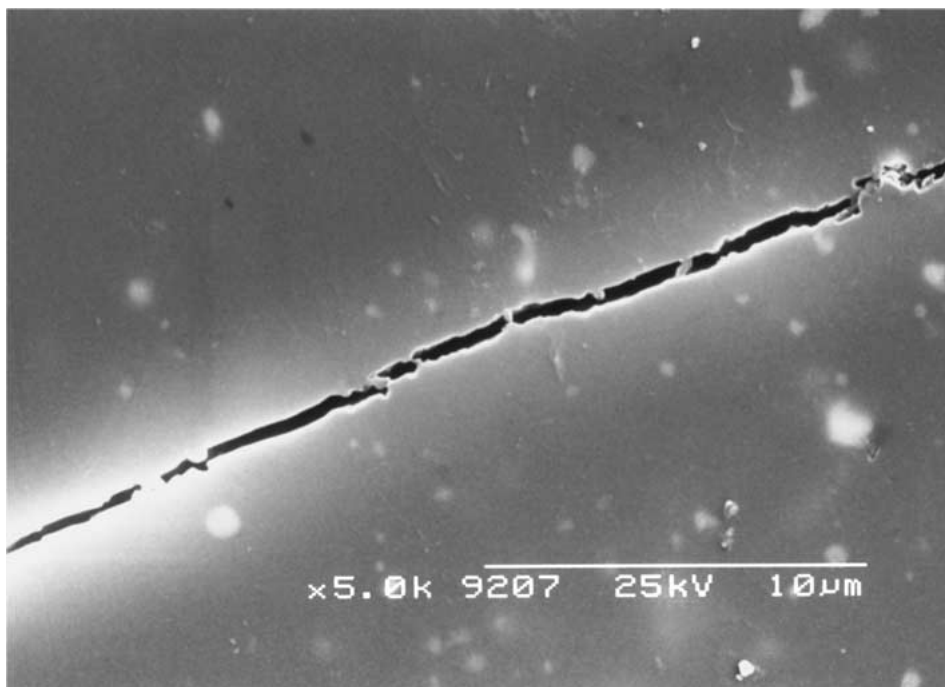
also be the result of the presence of a low-toughness interface or cleavage. There are three factors which affect crack deflection:

Firstly, the volume of elongated grains in the  $\alpha$ -sialon ceramic. For crack deflection, the first model of crack deflection proposed by Faber and Evans [2, 3] was based on a geometrical treatment of a crack deflecting from its main crack plane. According to the results of Faber and Evans [2, 3], the majority of the toughening from crack deflection appears to develop for a volume fraction of reinforcement of  $<0.2$  for a given shape of

particle. The toughness increase mainly arises from an increase in fracture surface area, changing the fracture mode from easy mode I to the more difficult modes II or III. From the microstructures (Figs 1c, 4c and 5c), it is estimated that the content of elongated  $\alpha$ -sialon grains in (1.0, 2.0) samples is about 20%; and that of elongated  $\beta$ -sialon grains in (0.5, 2.0) samples is about 40% although the total  $\beta$  phase content is about 60% according to XRD analysis. So, the contribution of the volume fraction of elongated grains in these two samples to crack deflection is very similar.

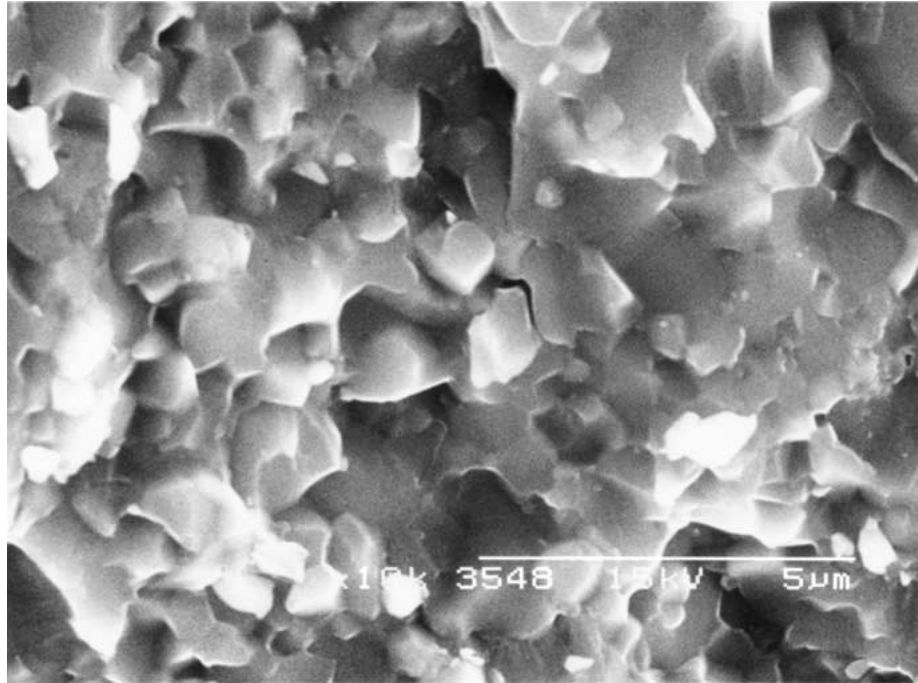


(a)



(b)

Figure 3 SEM micrographs of the indentation (a), crack propagation (b) and fracture surface (c) in the (1.0, 1.0) sample made from  $\beta$  rich  $\text{Si}_3\text{N}_4$  starting powders (Continued).



(c)

Figure 3 (Continued).

Secondly, the aspect ratio of the elongated grains. The average aspect ratio ( $L/D$ ) of the elongated  $\beta$ -sialon grains in sample (0.5, 2.0) is about 10–12, which is higher than that of elongated  $\alpha$ -sialon grains in (1.0, 2.0) samples with an average  $L/D$  of  $\sim 6$ . It was predicted that rod-shaped obstacles with large aspect ratios impart maximum toughness because high respect ratios result in a large twist angle of the crack. The maximum effect which can be achieved with rod-like particles is:

$$G_c/G_m \approx 4.0 \left( \text{when } \frac{L}{D} = 12 \right) \quad (3)$$

$$G_c/G_m \approx 3.0 \left( \text{when } \frac{L}{D} = 3 \right) \quad (4)$$

where  $G_c$  is the crack resistance force of the composite, and  $G_m$  the crack resistance force of the matrix. Therefore, the contribution of the elongated  $\beta$ -sialon grains in the (0.5, 2.0) sample to the fracture toughness is  $\sim 1.2$  times higher than that of elongated  $\alpha$ -sialon grains in (1.0, 2.0) samples according to the aspect ratio.

The last factor influencing crack deflection is the effect of thermal and Young's modulus mismatches. As described above, the Faber and Evans model [2, 3] ignored the local stress field at or near the interface between the matrix and the reinforcing phase, which is not quite consistent with published results. Actually, in the present work, there is another toughening mechanism which is the effect of the thermal residual stress field caused by thermal and elastic mismatches between the matrix and the reinforcing phase. Because the elongated  $\alpha$ - and  $\beta$ -sialon grains have different thermal expansion coefficients and slightly different Young's moduli, different local stress fields will form around the elongated grains, and these will play a large role in the crack deflection process. Assuming plane strain and

isotropic elastic behaviour, the thermal residual stress can be estimated according to Budiansky *et al.* [23] and Giannakopoulos *et al.* [24] analysis. Since the hot-pressing sintering temperature is higher than the matrix critical temperature  $T_c$  (i.e. the temperature below which the matrix ceases to behave viscoplastically), the change of temperature responsible for the thermal residual stress is

$$\Delta T = T_{\text{ambient}} - T_c \quad (5)$$

For temperatures above  $T_c$ , the matrix deforms plastically without imposing any residual stress on the elongated grains. The mismatch due to the thermal strain is:

$$\varepsilon = (\alpha_{el} - \alpha_{eq})\Delta T \quad (6)$$

Therefore the elongated grains and equiaxed  $\alpha$ -sialon interfacial pressure is:

$$P = E_{eq}(1 - f)\varepsilon/[2\lambda_1(1 - \nu_\alpha)] \quad (7)$$

where  $f$  is the volume fraction of the elongated grains, and shows that multiphase sialon ceramics generally have higher fracture toughness but lower hardness; the higher fracture toughness is because of the substantial amount of *in situ* growth of whisker-like  $\beta$ -sialon grains (see Fig. 1c). If  $\alpha_{el}$  and  $\alpha_{eq}$  are the linear thermal expansion coefficients, and if  $E_{eq}$  and  $E_{el}$  are Young's moduli, and  $\nu_{eq}$  and  $\nu_{el}$  are Poisson's ratios, with the subscripts el and eq referring to the elongated and equiaxed sialon grains, respectively, then in the case where  $\nu_{eq} = \nu_{el} = \nu$ :

$$\lambda_1 = 1 - (1 - 2\nu)[1 - f + (1 - f)E_{eq}/E_{el}]/[2(1 - \nu)] \quad (8)$$

and residual stress increases linearly from the sintering temperature down to the ambient temperature. It can be seen that the stresses are proportional to the difference between the thermal expansion coefficients of the equiaxed and elongated sialon grains. Although crack deflection caused by the residual stress field is different from that caused by the direct interaction between the crack and the elongated grains, residual stress plays a large role in the deflection process since it actually determines the type of crack-microstructure interactions.

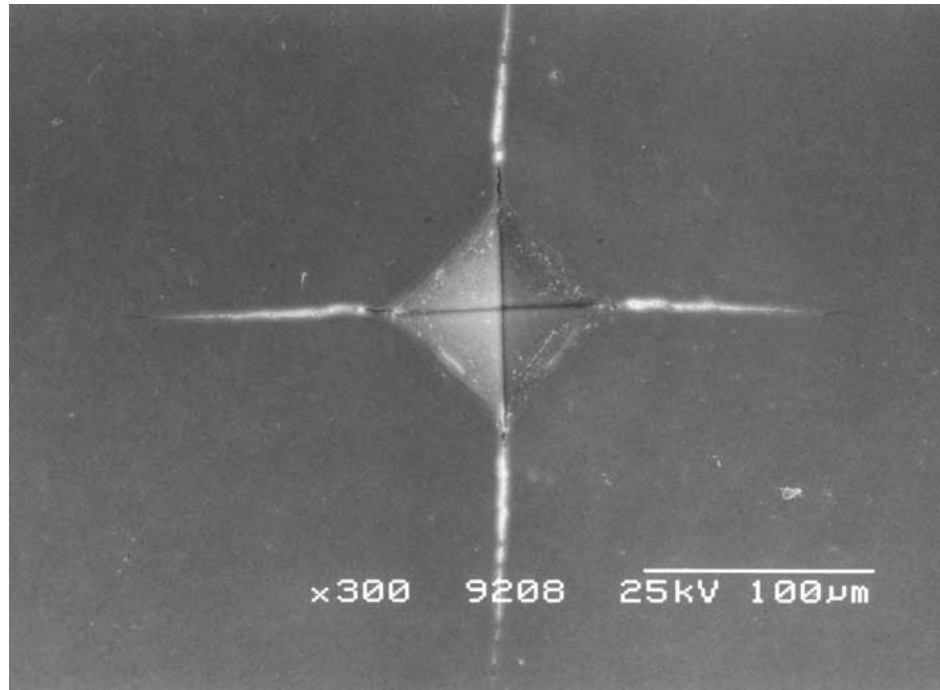
In the present study, in the (1.0, 2.0) samples consisting of pure  $\alpha$ -sialon ceramics reinforced with *in situ* formed elongated  $\alpha$ -sialon grains, the local residual

stress induced by thermal and elastic mismatch around the elongated  $\alpha$ -sialon grains is nearly zero, because the differences in the thermal expansion coefficient and Young's moduli between the matrix, equiaxed  $\alpha$ -sialon grains ( $\alpha_{eq\alpha}$ ,  $E_{eq\alpha}$ ) and the elongated grains ( $\alpha_{el\alpha}$ ,  $E_{el\alpha}$ ) are nearly zero, i.e.

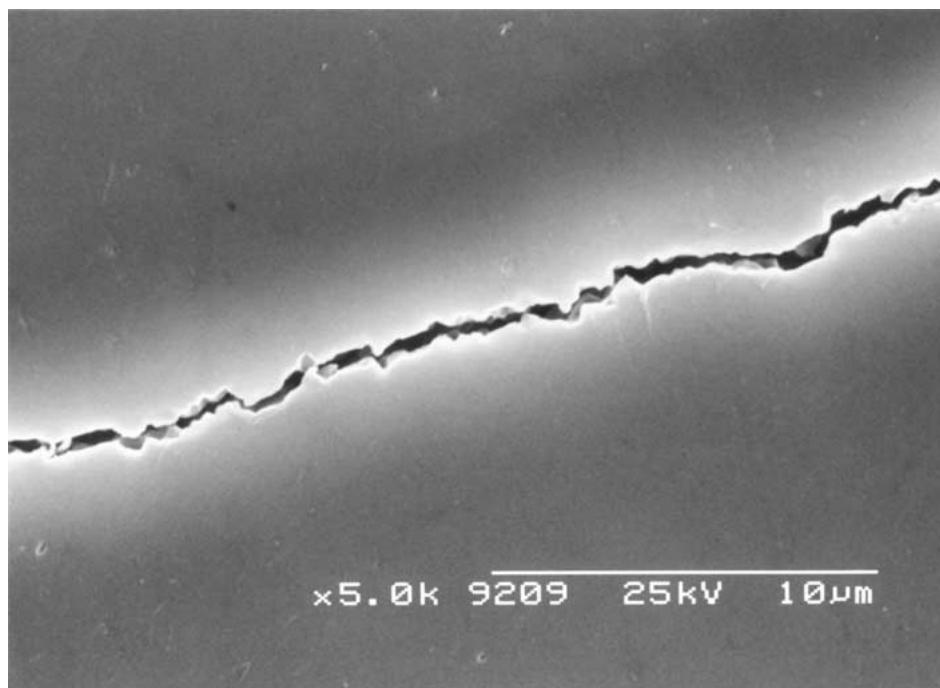
$$\Delta\alpha = \alpha_{el\alpha} - \alpha_{eq\alpha} = 0 \quad (9)$$

$$\Delta E = E_{el\alpha} - E_{eq\alpha} = 0 \quad (10)$$

So, the residual stress field makes little contribution to the crack deflection in (1.0, 2.0) samples, and

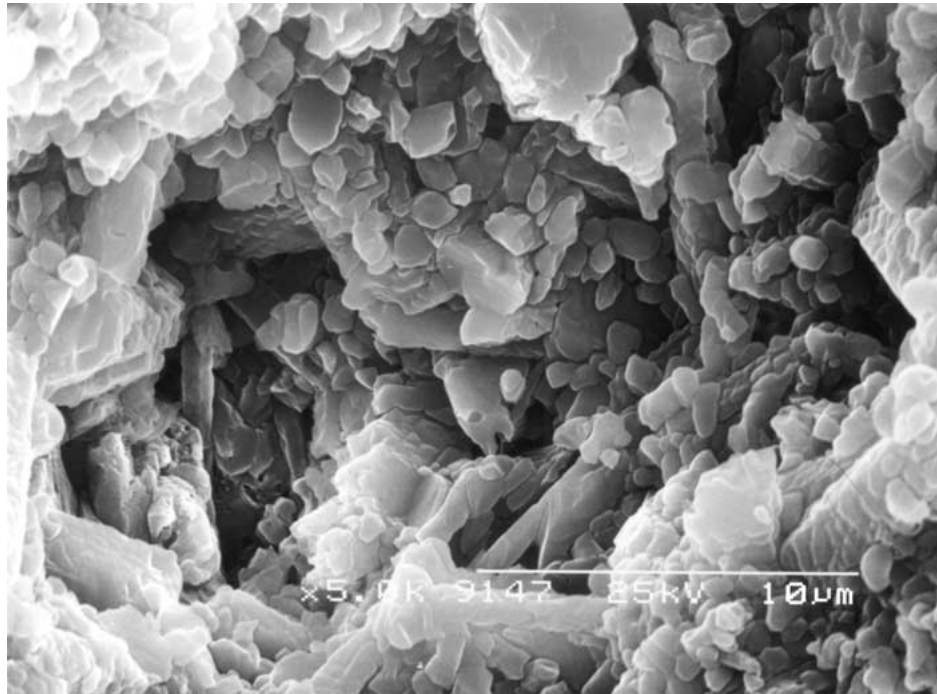


(a)



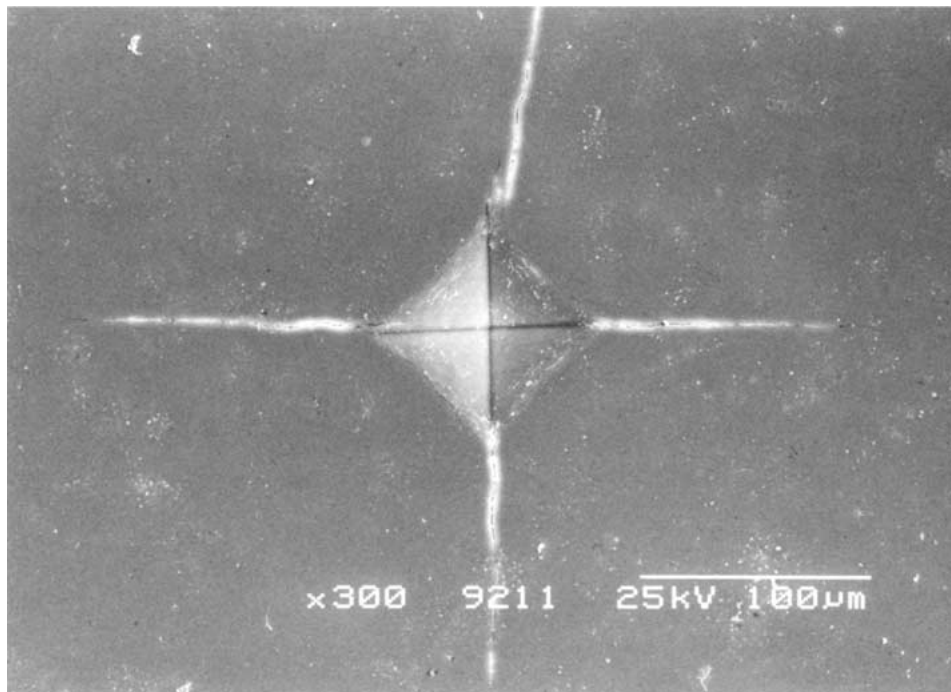
(b)

Figure 4 SEM micrographs of indentation (a), crack propagation (b) and morphology of grains (c) in the (1.0, 2.0) sample made from  $\alpha$  rich  $\text{Si}_3\text{N}_4$  starting powders (Continued).



(c)

Figure 4 (Continued).



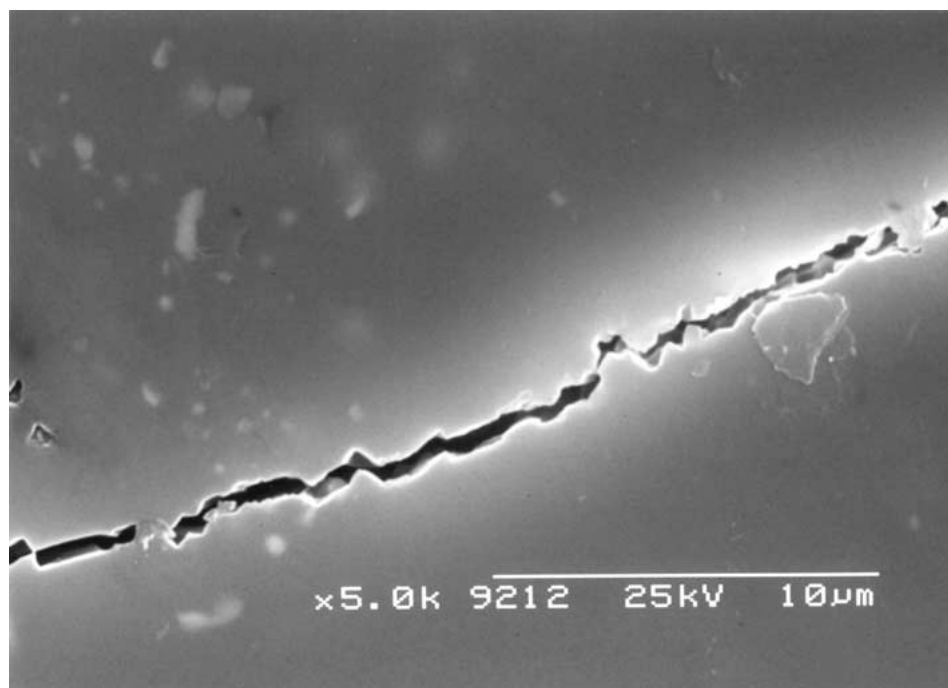
(a)

Figure 5 SEM micrographs of indentation (a), crack propagation (b) and morphology of grains (c) in the (1.0, 2.0) sample made from  $\beta$  rich  $\text{Si}_3\text{N}_4$  starting powders (Continued).

the amount of crack tilting and twisting is relatively small because this is only caused by the elongated grains.

However, in the two-phase  $\alpha/\beta$  (0.5, 2.0) sample, which consists of  $\alpha$ -sialon ceramics reinforced with *in situ* formed elongated  $\beta$ -sialon grains, there exists local residual stresses around the elongated  $\beta$ -sialon grains induced by thermal and elastic mismatch, because the thermal expansion coefficients and

Young's moduli between the matrix, equiaxed  $\alpha$ -sialon grains ( $\alpha_{\text{eq}}$ ,  $E_{\text{eq}}$ ) and the elongated grains ( $\alpha_{\text{el}\beta}$ ,  $E_{\text{el}\beta}$ ) are different. The mismatch in Young's modulus between  $\alpha$ -sialon ( $E_{\text{eq}\alpha} \cong 300\text{--}310$  GPa) and  $\beta$ -sialon ( $E_{\text{el}\beta} = 300\text{--}310$  GPa) is very small, and can be considered to be effectively zero; however, the thermal mismatch has a larger effect. As reported,  $\alpha$ -sialons have linear thermal expansion coefficients of about  $(3.4\text{--}4.0) \times 10^{-6} \text{C}^{-1}$  in the range from room temperature



(b)



(c)

Figure 5 (Continued).

to 1400°C [25–27], whereas,  $\beta$ -sialon ceramics have linear thermal expansion coefficients of about  $(2.7\text{--}3.4) \times 10^{-6} \text{ } ^\circ\text{C}^{-1}$  in the temperature range 25–1000°C, i.e.  $\Delta\alpha = \alpha_{\text{el}\beta} - \alpha_{\text{eq}\alpha} < 0$ , because the  $\beta$ -sialon expansion is smaller than that of  $\alpha$ -sialon. Therefore, the elongated  $\beta$ -sialon phase will be under compressive stress, and the interfacial pressure between  $\alpha$  and  $\beta$  grains can be estimated to be as high as 290 MPa. From the crack propagation behaviour in two-phase  $\alpha/\beta$  (0.5, 2.0) samples (Fig. 1b), crack deflection round the elongated  $\beta$  grains is the main toughening mechanism, so, when the crack propagates, more energy will

be needed to overcome the additional compressive force caused by the thermal mismatch between the two different phases. Therefore apart from the contribution of elongated grains, the residual stress field in the (0.5, 2.0) two-phase sample also makes some contribution to crack deflection as well. So the crack tilting and twisting are more marked in the (0.5, 2.0) sample than in the (1.0, 2.0) sample and so is the fracture toughness. This is why in the present work  $\alpha$ -sialon samples reinforced by *in situ* formed  $\beta$ -sialon needles have a higher  $K_{\text{Ic}}$  than similar samples reinforced by elongated  $\alpha$ -sialon grains.

#### 4. Conclusions

Self-reinforcement of Li- $\alpha$ -sialon ceramics can be achieved by the presence of either elongated  $\beta$ -sialon or  $\alpha$ -sialon grains. Microscopy studies reveal that particle debonding, pullout and crack deflection all contribute towards the reinforcement mechanism. Crack deflection is not only determined by the morphology of the elongated grains; thermal mismatch and elastic mismatch between the equiaxed  $\alpha$ -sialon grains and the elongated grains also have a strong impact on crack deflection and hence the fracture toughness. From the present study, It is believed that  $\alpha$ -sialon ceramics reinforced with elongated  $\beta$ -sialon grains have more advantages than when reinforced with elongated  $\alpha$ -sialon grains because of the more favourable crack deflection toughening mechanisms involved.

#### Acknowledgements

The authors would like to thank the Defence Evaluation and Research Agency for financial support.

#### References

1. A. J. PYZIK and A. M. HART, in "Phase Diagram in Advanced Ceramics," edited by A. M. Alper (Publ. Academic Press, Inc., 1995) p. 159.
2. K. T. FABER and G. EVANS, *Acta Metall.* **31**(4) (1983) 565.
3. *Idem.*, *ibid.* **31**(4) (1983) 577.
4. M. M. SEABAUGH, I. H. KERSCHT and G. L. MESSING, *J. Amer. Ceram. Soc.* **80**(5) (1997) 1181.
5. V. S. STUBICAN and R. C. BRADT, *Ann. Rev. Mater. Sci.* **11** (1981) 267.
6. F. F. LANGE, *Int. Met. Rev.* **25**(1) (1980) 1.
7. G. WOTTING, B. KANKA and G. ZIEGLER, in "Non-oxide Technical and Engineering Ceramics," edited by S. Hampshire (Elsevier, London and New York, 1986) Ch29, p. 83.
8. T. EKSTRÖM, *Mater. Sci. Eng.* **A109** (1989) 341.
9. H. MANDAL, D. P. THOMPSON and T. EKSTRÖM, *J. Eur. Ceram. Soc.* **12** (1993) 421.

10. T. EKSTRÖM, "Engineering Ceramics'96: Higher Reliability Through Processing" (Kluwer Academic Publishers, 1997) p. 147.
11. D. P. THOMPSON, in "Tailoring of Mechanical Properties of Si<sub>3</sub>N<sub>4</sub> Ceramics," edited by M. J. Hoffmann and G. Petzow (Kluwer, Academic Publishers, The Netherlands, 1994) p. 125.
12. Z. B. YU, D. P. THOMPSON and A. R. BHATTI, *J. Eur. Ceram. Soc.* 2000, in press.
13. Z. J. SHEN, *et al.*, in "Engineering Ceramics'96 : Higher Reliability through Processing," edited by G. N. Babini *et al.* (Kluwer Academic Publishers, 1997) p. 169.
14. H. ZHAO, S. P. SWENSER and Y. -B. CHENG, *J. Eur. Ceram. Soc.* **18** (1997) 1053.
15. C. A. WOOD, H. ZHAO and Y. -B. CHENG, *J. Amer. Ceram. Soc.* **82**(2) (1999) 421.
16. I. W. CHEN and A. ROSENFLANZ, *Nature* **389** (1997) 701.
17. Z. B. YU, D. P. THOMPSON and A. R. BHATTI, *in situ* growth of elongated  $\alpha$ -sialon grains in Li- $\alpha$ -sialon ceramics, to be published.
18. A. G. EVANS, M. RUHLE, B. J. DALGLEISH and M. D. THOULESS, "Advanced Structural Ceramics" (1987) Ch30, p. 259.
19. A. G. EVANS, *J. Amer. Ceram. Soc.* **73**(2) (1990) 187.
20. P. F. BECHER, *ibid.* **74**(2) (1991) 255.
21. Z. B. YU, D. P. THOMPSON and A. R. BHATTI, *British Ceram. Trans.* **97**(2) (1998) 41.
22. A. G. EVANS and A. CHARLES, *J. Amer. Ceram. Soc.* **59**(7/8) (1976) 371.
23. B. BUDIANSKY, J. W. HUTCHINSON and A. G. EVANS, *J. Mech. Phys. Solids* **43**(2) (1986) 167.
24. A. E. GIANNAKOPOULOS and K. BREDER, *J. Amer. Ceram. Soc.* **14**(1) (1991) 194.
25. K. H. JACK, in "Progress in Nitrogen Ceramics," edited by F. L. Riley (NATO, ASI Series, E65, Martinus Nijhoff, The Hague, 1983) p. 450.
26. H. K. PARK, D. P. THOMPSON and K. H. JACK, "Science of Ceramics," edited by H. Hausner (DKG, Weiden, 1980) vol. 10, p. 251.
27. M. MITOMO, F. IZUMI, P. GREIL and G. PETZOW, *Amer. Ceram. Soc. Bull.* **63** (1984) 730.

Received 1 November 2000  
and accepted 14 February 2001